

TSF0013

## The Effects of Detached Baffles that Impacts Heat Transfer and Friction Behaviors within parallel plates

Arnut Phila<sup>1,\*</sup>, Smith Eiamsa-ard<sup>2</sup>, and Chinaruk Thianpong<sup>1</sup>

<sup>1</sup> Department of Mechanical Engineering, Faculty of Engineering, King Mongkut's Institute of Technology Ladkrabang,  
1 Chalongkrung Road, Ladkrabang, Bangkok, Thailand, 10520

<sup>2</sup> Department of Mechanical Engineering, Faculty of Engineering, Mahanakorn University of Technology,  
140 Cheum-Sampan Road, Nongchok, Bangkok 10530

\* Corresponding Author: Email: arnut\_phila@hotmail.com, Tel.: (+66)86-506-6564

### Abstract

This research has its aim to introduce the study upon the characteristics of heat transfer and friction for turbulent flow within the parallel plate under a constant heat flux state at the lower wall. The detached baffles were installed at the plate's lower wall where the placement of the baffles is purposed to block air flow. The height of the detached baffles ( $e$ ) equals to 6 millimeters in which owns a blockage ratio ( $BR$ ) of 0.15 with a gap between the baffles that equals to 60 millimeters and its relative roughness pitch ( $P/e$ ) of 10. Modifications to the floating distance of the baffles have been made as follows: 0, 2, 4, 6, 8, and 10 millimeters, where the ratio of the floating distance of the baffles over the parallel plate's height; ( $b/H$ ) equals to 0, 0.05, 0.10, 0.15, 0.20 and 0.25. Considering an experiment with a plane tube, air as a fluid will be required to work at Reynolds number ( $Re$ ) starting from 9,000 to 24,000 to study and consider the value of heat transfer in a form of Nusselt number ( $Nu$ ) and pressure loss in a form of friction factor ( $f$ ), where the results of the experiment will be compared to the plane parallel plates. The results have proved the detached baffles to have a floating distance of 0 millimeters, giving off heat transfer values and friction factor higher than that of the detached baffles with floating distance of 2, 4, 6, 8, and 10 millimeters. On the other hand, thermal enhancement factor ( $\eta$ ) in the case of detached baffles with floating distance of 0 millimeters and Reynolds number of 9,000, gives off the highest value of 1.31 and is considered higher in value under all conditions within the experiment's conduction.

**Keywords:** Channel flow, detached baffles, heat transfer enhancement.

### 1. Introduction

In the present, the industry has applied and adapted the use of heat exchangers in various engineering fields like reactors, boilers, evaporators, condensers, and including computer CPU cooling methods. Most engineers and heat exchanger developers often regard the price and heat transfer efficiency as the major factor and as well regard if they meet the specifications required by the industrial sector [1-3]. The common techniques used to test the efficiency of heat exchangers are divided into 3 techniques: (1) Active method- a technique that requires external energy to aid in heat transfer (eg--> pulsation by cams [4], mechanical aids [5], surface and fluid vibration [6], suction or injection [7] and electrostatics fields [8]), (2) Passive method- a technique that designs and modifies the characteristics of the heat transfer channel structure (eg--> treated surface [9] rough surface [10], extended surface [11], swirl flow device [12] and additives for fluid and gas [13]), and (3) Compound method- a technique that combines both the active method together with the passive method (eg--> rough surface with twisted tapes [14] and rough surface with fluid vibration [15]). Nevertheless, Passive method is considered the most suitable method to enable the increase in heat transfer efficiency which can be observed through various research conducts and studies that have been widely

published. Pongjet et al. [16], for instance, has examined the behaviors of heat transfer and the friction of fluids in heat exchange channels installed with numerous baffle types. The study has found that the coefficient of heat transfer, including the friction factor, have had higher values than smooth surfaced channels. The wedge rib pointing downstream baffle gave off the highest value in terms of heat transfer efficiency and friction. Nevertheless, the triangle rib with staggered array baffle has the highest thermal performance index value compared to all cases that have been studied and tested. Kumar et al. [17] has conducted a study to experiment heat transfer and pressure drop in a solar air heater that has been installed with discrete W-shaped roughness in a rectangular channel with aspect ratio of 8:1. The experiment has been done with Reynolds number between 3,000 to 15,000, where the relative roughness pitch has been controlled to remain stable at 10, then relative roughness height has been changed between 0.0168 to 0.0338 and the angle of attack value between 30 to 75 degrees. The study has found that changes in various parameters have influenced the heat transfer efficiency and friction factor, making the values higher in all causes within the study once compared to smooth surfaced channels. Sriharsha et al. [18] has reported the results of the study upon the effects of installing the 90° continuous and 60° V-Broken ribs

## TSF0013

within a rectangular channel between Reynolds number of 10,000 to 30,000. The results have shown that heat transfer within a rectangular channel installed with 90° continuous attached ribs had an increase in value when the rib height to hydraulic diameter ratio is higher. On the contrary, the pressure drop rose. Installed 60° V-Broken ribs resulted in higher value of heat transfer compared to the 90° continuous ribs, where it as well resulted in much lower pressure drop.

From past conducted researches, more studies have been conducted to learn of heat transfer capacity when installed with numerous baffles in various forms. The objective of installing baffles is to enable fluid impingement and the formation of a stream line, which will lead to recirculation at the area behind the baffles (acceleration region) and as well lead to the reattachments of fluids at the channel surface which will enable an increase in heat transfer value. However, the area right behind the baffles is a low-heat transfer area due to the slow-passing motion of fluids at the area behind the baffles, resulting in low heat transfer ratio.

Therefore, this research article aims to modify heat transfer at the area around the baffles by installing the baffles with floating distance from the below surface/wall. The objective is to enable air and its entrance to result in an impingement at the area behind the baffles to obtain higher heat transfer values and reducing pressure drop with Reynolds number between 9,000 to 24,000.

### 2. Roughness parameters

The roughness parameters of the detached baffles are determined by baffle height ( $e$ ), baffle pitch ( $P$ ), floating distance of the baffles ( $b$ ) and parallel plate's height ( $H$ ). These parameters have been converted in the form of the following dimensionless parameters:

- (i) Relative roughness pitch, ( $P/e$ ).
- (ii) Relative roughness height, ( $e/H$ ).
- (iii) Relative roughness floating term, ( $b/H$ ).

The scope of these dimensionless quantities and other parameters employed in this investigation are presented in "Fig. 1" and Table. 1.

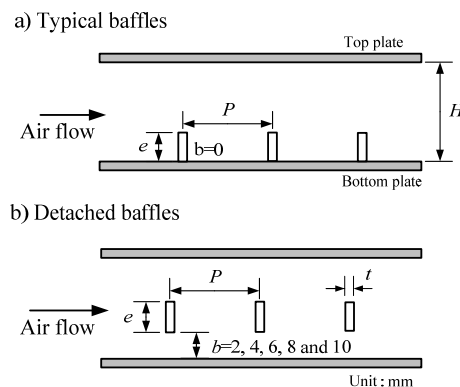


Fig. 1. Test section with baffle inserts: (a) typical baffles (b) detached baffles.

Table. 1. Dimensionless quantities and other parameters used in experiments of test channel experiments.

Test section	
Height of test channel, $H$ (mm)	40
Width of test channel, $W$ (mm)	150
Length of test channel, $L$ (mm)	600
Aspect ratio, $AR$	3.75
Baffle	
Material	PLA Plastics
Thickness of baffle, $t$ (mm)	1
Height of baffle, $e$ (mm)	6
Width of baffle, $l$ (mm)	150
Free-spacing Length, $P$ (mm)	60
Height of floating baffle, $b$ (mm)	0, 2, 4, 6, 8 and 10
Test condition	
Working fluid	Air
Reynolds number, $Re$	9,000 to 24,000
Prandtl number, $Pr$	0.7

### 3. Experimental program

#### 3.1 Experiment setup

The equipments used in the conducted research are as illustrated in "Fig. 2". A fan with 3 horsepower has been installed as the source of air flow, in which the entrance of air can be controlled with an inventor through the use of an orifice meter which measures the flow rate [19]. The air compressed by the fan will pass through a 1800 millimeters long channel to adapt the flow, turning it into a fully development flow before entering the test section and has been designed according to the suggestion of Ower & Pankhurst [20] to prevent the separation of cross-sectioning of the flow within the test channel. Within the test channel, a sheet heat coiled wire that gives off stable electricity of 40 watts has been installed where RTD Pt100 temperature measuring equipment has been used to measure the temperature of air, both entrance and exit flows. Also, a comparative temperature tested Thermochromic liquid crystal sheet has been used to measure the temperature on the surface of the test channel to enable the distribution of temperature on the surface with heat transfer. Pressure drop can be measured with Pressure differential transmitters; the entire experimental equipments have been covered with insulators to prevent heat loss.

#### 3.2 Experimental procedure

Before the experiment, RTD Pt100, an equipment used to measure temperature, has its correctness examined carefully while the system's leakage and pressure drop measuring area at various locations have been checked. The experiment has been done in a steady-state condition to collect crucial data required for the findings of heat transfer coefficient and friction factor.

The steady state conditions of the flow will specify the changes of temperature at different measuring areas to remain stabilized for 15 minutes. Once the conditions of the experiment have been changed, it is required to wait for the flow to return to

## TSF0013

its initial, stabilized state once again, which would probably need around 20-30 minutes of time. Each condition of experiment requires heat flux constant controlled. After the latter has been done, the mass flow rate has been modified; then, it is required to wait for the flow to return to its stable condition in order to record the data of values obtained from the experiment. Photos of Thermochromic liquid crystal sheets were taken, where the measured parameter values are as follows:

- (i) Temperature of electrical heating plate obtained from thermochromic liquid crystal surface.
- (ii) The inlet and outlet temperatures of air.
- (iii) Pressure drop across the test section and the orifice meter.
- (iv) Voltage provided and current flow through in the electrical heating plate.

### 3.3 Data reduction

Data of heat surface plate and air temperatures in the channel tube at different points in a steady state were used to determine the values of final parameters, namely heat transfer coefficient ( $h$ ) and friction factor ( $f$ ), which were calculated as:

The Reynolds number based on the hydraulic diameter of test section is given by

$$Re = \frac{V_i D_h}{\nu} \quad (1)$$

where  $D_h$  is the hydraulic diameter of test section (m),  $\nu$  is the kinematics viscosity of air ( $m^2/s$ ) and  $V_i$  is the inlet air velocity (m/s).

Mass flow rate is calculated by,

$$\dot{m} = \rho A_x V_i \quad (2)$$

where  $\rho$  is the density at bulk air temperature ( $kg/m^3$ ) and  $A_x$  is the cross sectional area of test section ( $m^2$ ).

The total heat sourced by the electrical heating plate is calculated as,

$$Q_e = V_e I \quad (3)$$

where  $V_e$  is the voltage provided (V) and  $I$  is the current flow through in the electrical heating plate (A).

Heat loss ( $Q_{loss}$ ) straight through the insulation, is calculated by measuring the average wall temperatures and the ambient air temperatures, estimated as 1–3% of the total heat sourced.

Therefore, the actual heat sourced by the electrical heating plate is

$$Q_1 = Q_e - Q_{loss} \quad (4)$$

and heat absorbed by the fluid is calculated as,

$$Q_2 = \dot{m} C_p (T_o - T_i) \quad (5)$$

where  $C_p$  is the specific heat capacity of air (J/kg K), and  $T_i$  and  $T_o$  are the inlet and outlet air temperatures (K), respectively.

Heat balance between the actual heat sourced ( $Q_1$ ) and the heat absorbed by the fluid ( $Q_2$ ) was within 1–5% for all tested. The heat transfer rate ( $Q$ ) was calculated from the actual heat sourced by electrical heating plate and the heat absorbed by the fluid for convective heat transfer computation.

Therefore it is expressed as follows:

$$Q = \frac{Q_1 + Q_2}{2} \quad (6)$$

and the heat flux was calculated by,

$$q = \frac{Q}{WL} \quad (7)$$

where  $W$  is the width of electrical heating plate (m) and  $L$  is the length of the tube (m).

Local convective heat transfer coefficient can be evaluated from,

$$h_x = \frac{q}{(T_{wx} - T_{bx})} \quad (8)$$

where  $T_{bx}$  and  $T_{wx}$  are the local bulk air and thermochromic liquid crystal surface temperatures (K), respectively.

The local bulk air temperatures is calculated by the following energy balance equation,

$$T_{bx} = T_i + \frac{qwx}{\dot{m}C_p} \quad (9)$$

where  $w$  is the wetted perimeter (m) and  $x$  is the local distance of the parallel plates (m).

The local Nusselt number is evaluated by:

$$Nu_x = \frac{h_x D_h}{k} \quad (10)$$

where  $k$  is the thermal conductivity of air (W/m K).

The average heat transfer coefficient is determined from,

$$h = \frac{q}{(T_w - T_b)} \quad (11)$$

where  $T_b$  and  $T_w$  are the mean bulk air and thermochromic liquid crystal surface temperatures (K), respectively.

The average Nusselt number is written as:

$$Nu = \frac{h D_h}{k} \quad (12)$$

and the friction factor is evaluated by:

$$f = \frac{\Delta P}{\left(\frac{L}{D_h}\right) \left(\rho_o \frac{V^2}{2}\right)} \quad (13)$$

where  $\Delta P$  is the pressure drop across the test section ( $N/m^2$ ).

TSF0013

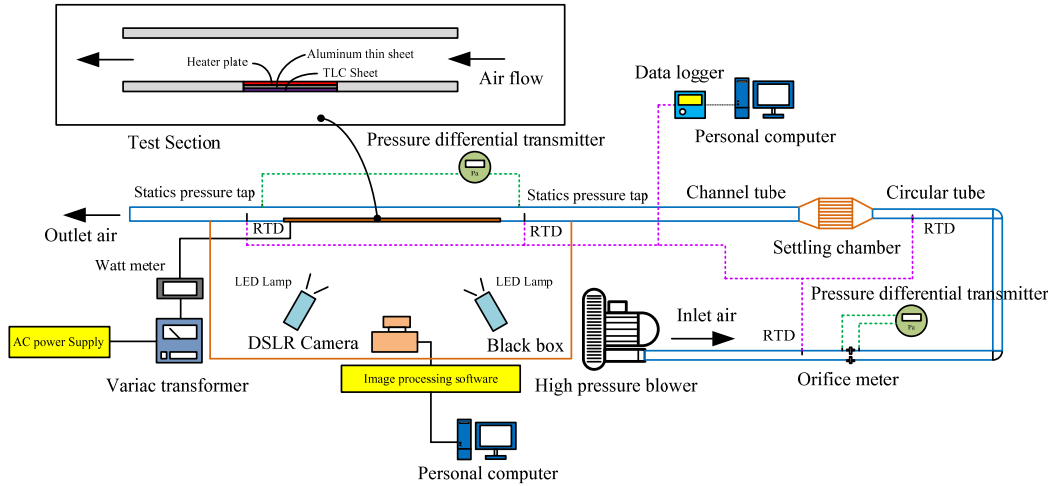


Fig. 2. Schematic diagram of experiment apparatus.

For a constant pumping power, the thermal enhancement factor ( $\eta$ ) is defined as the ratio of the heat transfer coefficient of the parallel plates with detached baffles ( $h$ ) to that of the smooth channel without detached baffles ( $h_0$ ).

$$\eta = \frac{h}{h_0} = \left( \frac{Nu}{Nu_0} \right) \left( \frac{f}{f_0} \right)^{-1/3} \quad (14)$$

where  $h_0$  is the convective heat transfer coefficient for the smooth channel ( $W/m^2 K$ ), and  $Nu_0$  and  $f_0$  are the Nusselt number and friction factor of smooth channel, respectively.

#### 4. Results and discussion

This conducted research has studied the installment of detached baffles which affects the behavior of heat transfer coefficient, friction factor, and efficiency in enabling heat transfer. The experiment has been conducted, where modifications have been made to the floating distance of baffles ( $b$ ) as the following: 0, 2, 4, 6, 8 and 10 millimeters with ratio of floating distance and the parallel channel height ( $H$ ) of 0, 0.05, 0.10, 0.15, and 0.20 between Reynolds number of 9,000 into 24,000. The results of heat transfer coefficient and friction factor were both examined along with the standard coefficient value to use as a reference data in order to further analyze information regarding heat transfer in test channels.

##### 4.1 Validation of smooth channel: results

It may be noted that prior to actual data collection, the test setup was checked by conducting experiments for a smooth channel. The present Nusselt number and friction factor values of the smooth channel with the experimental correlation of Dittus Boelter and Blasius equation [21] under the same operation test conditions.

Dittus-Boelter equation:

$$Nu = 0.024 Re^{0.8} Pr^{0.4} \quad (15)$$

Blasius equation:

$$f = 0.085 Re^{-0.25} \quad \text{for } Re < 20,000 \quad (16)$$

$$f = 0.184 Re_d^{-0.2} \quad \text{for } Re \geq 20,000 \quad (17)$$

In this research report, heat transfer coefficient will be displayed in the form of Nusselt number values, while the pressure loss of the test channel will be displayed in the form of friction factor value. The smooth surfaced channel has its values confirmed with the standard coefficient values from the past study conducted by Dittus-Boelter for the Nusselt number values. While the friction factor has its values compared to Blasius.

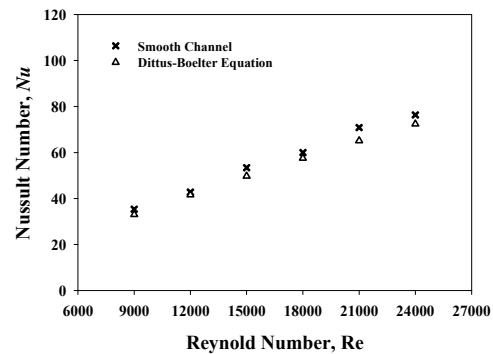


Fig. 3. Verification of Nusselt number values for smooth channel.

“Figs. 3 and 4” have shown the results of the experiment when compared to the standard coefficient values obtained from smooth surfaced channels, where the values are quite similar to each other. The difference value of the data is less than  $\pm 6\%$  and  $\pm 4\%$  for the Nusselt number values and friction factor accordingly. The results of this study have shown the correctness of equipment installation and techniques upon measurement used in this experiment [22].

## TSF0013

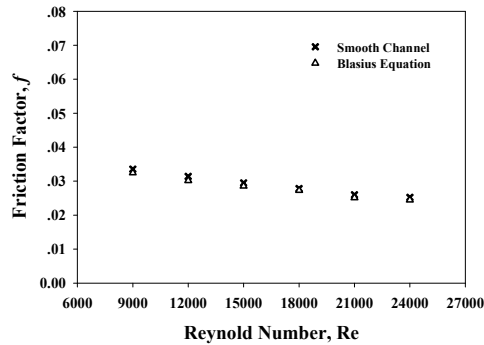


Fig. 4. Verification of friction factor values for smooth channel.

### 4.2 Flow structure and temperature field: Results

The flow pattern and distribution of Nusselt number in the channel tube with detached baffles of different distance (height of the detached baffles) ( $b=0, 2, 4, 6, 8$  and  $10$ ) is shown in “Fig. 5”.

The air flow and distribution of Nusselt number values in this conducted research will be displayed at the Reynolds number of  $Re=24,000$  with floating

distance of the baffles equal to  $b=0, 2, 4, 6, 8,$  and  $10$  millimeters. From the graph in “Fig. 5(a) into 5(f)”, the floating distance of the baffles equals to  $b=0$ , which resulted in large recirculation zone at the area behind the baffles (acceleration region). However, when the floating value is increased, recirculation zone decreases in value (de-acceleration region) until the floating distance value of the baffles exceed 4 millimeters ( $b=4, 6, 8,$  and  $10$  millimeters), that the recirculation will not occur (recirculation is not found). The process in heat transfer of baffles in the area of recirculation is highly important as it affects the changes of Nusselt number values, where this process will result in better mixing of fluids between heat and air exchanging surface at the channel's core region.

From “Fig. 6”, it can be seen that the distance  $b=0$  gives off the best overall heat transfer value due to the increase in mixing fluids. Furthermore, the boundary layer becomes thinner in recirculation zone which differs from cases of other conditions (with high distance value of  $b$ ) as it does not result in recirculation at the area behind the baffles (acceleration region).

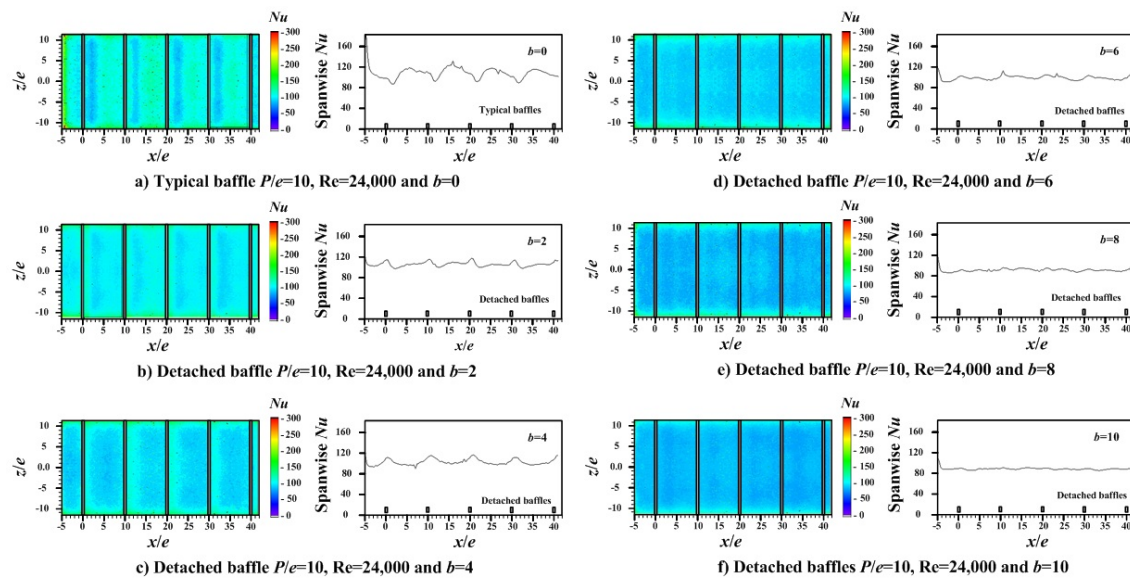


Fig. 5. Nusselt number distribution and spanwise average Nusselt number on the heat transfer surface: (a) typical baffles ( $b=0H$ ), (b-f) detached baffles ( $b=0.05H, 0.10H, 0.15H, 0.20H$  and  $0.25H$ ).

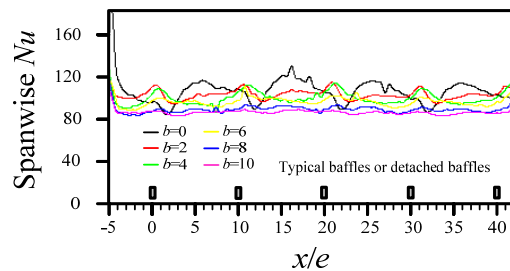


Fig. 6. Spanwise average Nusselt number on the heat transfer surface for various floating distance of baffles.

### 4.3 Influence of relative roughness floating term ( $b/H$ ): results

Heat transfer in rectangular channel installed with detached baffles in constant heat flux condition within this conducted research is displayed in the form of an image (or the term of) of Nusselt number values. The relationship between the Nusselt number values and Reynolds number ranging from 9,000 to 24,000 at different floating distance values is shown in “Fig. 7”. Generally, Nusselt number values will increase when Reynolds number increase as it raises higher turbulent intensity imparted values at areas between the baffles.



## TSF0013

In each every condition of the experiment (with installed baffles), the Nusselt number is higher than the condition of the smooth channel which shows that the increase in heat transfer resulted from the influence of baffles used in the installation.

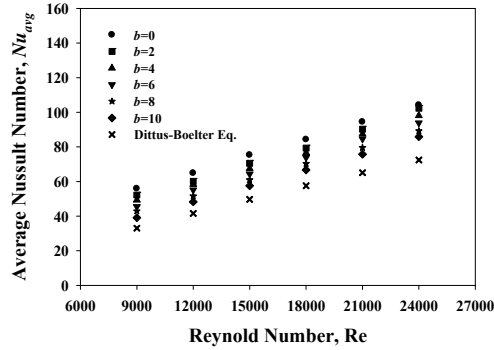


Fig. 7. Relationship between the Nusselt number and Reynolds number for various floating distance of baffles.

In the state of similar condition in experiments with an increase in floating distance of baffles ( $b$ ), the heat transfer ratio will be influenced and therefore decreased due to the formation of a recirculation zone or eddy motion at the acceleration zone, which decreases in value. However, recirculation zone will not be formed when ( $b$ ) exceeds 4 millimeters, which will result in the mixing of fluids at the channel surface and core region, plus, result in the formation of eddy motion between the baffles to have worse values.

Experimenting with floating distance of baffles at ( $b=0, 2, 4, 6, 8, \text{ and } 10$ ),  $b=0$  resulted in the highest values of Nusselt number and Reynolds number of 24,000. The average value of Nusselt number in the condition of baffles installment with floating distance at  $b=0, 2, 4, 6, 8, \text{ and } 10$  millimeters equals to 171.91%, 162.77%, 156.34%, 148.84%, 140.56%, and 132.42% accordingly, once compared to test channels without baffle installment.

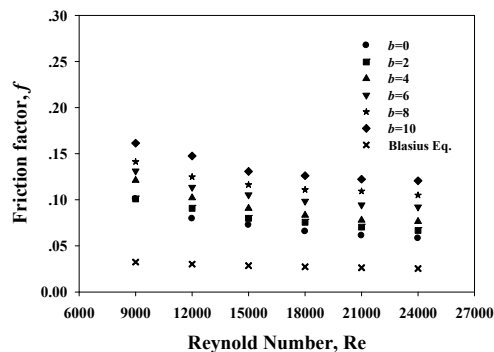


Fig. 8. Relationship between the friction factor and Reynolds number for various floating distance of baffles.

The effects of the floating term of the baffles on friction factor behavior is depicted in “Fig. 8”. As shown, the relationship between the friction factor and Reynolds number at different detached baffles for all test conditions. It could be shown that the friction factor ( $f$ ) was in the similar trend both for the smooth channel and the channel with detached baffles.

The friction factor value decreased when Reynolds number ( $Re$ ) increases.  $Re=9,000$  (low Reynolds number) greatly affected the friction factor. “Fig. 8” showed that the friction factor increased when the floating distance of baffles ( $b$ ) increases. As the height of the baffles increased, it blocked the core flow region which resulted in fierce impingement which led to the loss of momentum and resulted in changes of pressure that highly increased.

In the section with a condition that regarded the friction factor resulting from the detached baffles, the results revealed values ranged from 255.20 to 474.64 percents were the results, once compared to the smooth channel.

#### 4.4 Thermal performance criteria: results

“Fig. 9” presents the relationship between Reynolds number ( $Re$ ) and the Nusselt number ratio ( $Nu/Nu_0$ ), which is defined as the ratio of the Nusselt number of the detached baffles to the Nusselt number of a channel without the detached baffles. Nusselt number ratio decreases once the Reynolds number increases in the experimental section between 9,000 to 24,000. The average values of Nusselt number ratio ( $Nu/Nu_0$ ) for rectangular channel that has been installed with detached baffles in this experiment were at 1.31 to 1.91 for the changes in the floating distance at various locations.

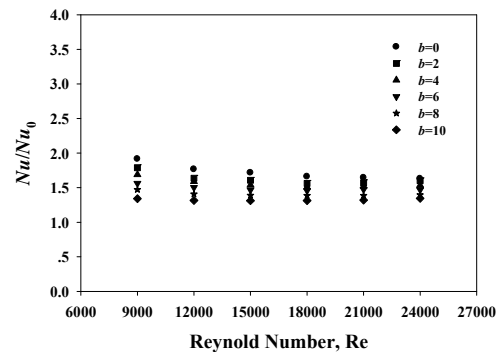


Fig. 9. Relationship between the Nusselt number ratio ( $Nu/Nu_0$ ) and Reynolds number.

Variation of friction factor ratio ( $f/f_0$ ) with Reynolds number is shown in “Fig. 10”. The experiment has shown that the trends of Nusselt number ratio ( $Nu/Nu_0$ ) will be similar to the trends of friction factor ratio ( $f/f_0$ ). The friction factor ratio obtained from the experiment was at 2.33 to 4.98.

## TSF0013

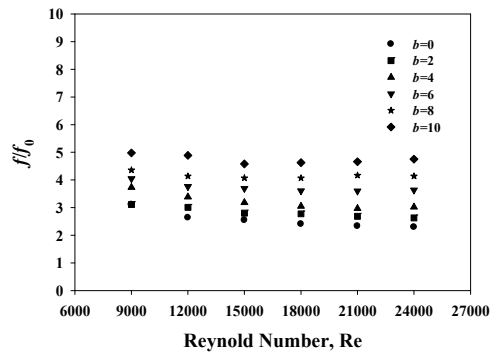


Fig. 10. Relationship between the friction factor ratio ( $f/f_0$ ) and Reynolds number.

“Fig. 11” presented the relationship between the thermal enhancement index and Reynolds number in a rectangular channel with detached baffles at several floating distance of the baffles. The graph of the experiment has shown that the thermal enhancement index value increases when Reynolds number decreases. It was noteworthy that the enhancement efficiency in a rectangular channel with detached baffles was 0.77 to 1.31 higher than those of the smooth channels under equal pumping power, since these are relevant to the operating cost.

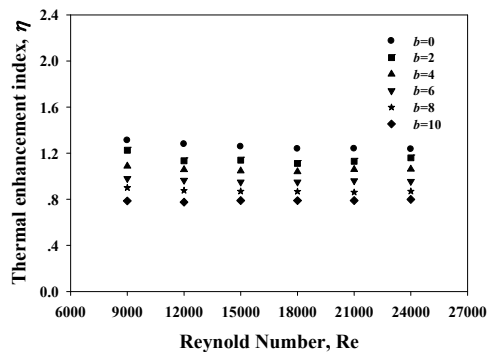


Fig. 11. Relationship between the thermal enhancement index and Reynolds number.

### 5. Conclusions

The impacts of the detached baffles with several floating distance of the baffles ( $b=0, 2, 4, 6, 8$  and  $10$  millimeter) on the heat transfer rate, friction factor and thermal performance index characteristics have been investigated experimentally for Reynolds numbers ranging from  $9,000$  to  $24,000$ . The use of detached baffles installed provided essential argumentation of heat transfer with a corresponding increase in friction factor. Based on the experimental data, goal findings of this study could be epitomized as follows:

- In general, it was found that the heat transfer and thermal enhancement index increased along with the decreasing floating term of the baffles. Conversely,

friction factor increases along with the increasing floating term.

- Low floating distance of the baffles ( $b=0$  and  $2$  millimeters) greatly influenced the behavior of heat transfer, friction factor, and thermal performance index as a result of recirculation zone or eddy motion which caused the mixing of fluids between the channel surface and the core region of fluids, further leading to the thinning of boundary layer.

- Floating distance of the baffles exceeding  $0$  ( $b>0$  millimeters) resulted in a decrease in recirculation zone and will not result in any formation of recirculation when the floating distance of baffles have values exceeding  $4$  millimeters ( $b>4$  millimeters), which resulted in a decrease in heat transfer.

- The Nusselt number ( $Nu$ ) was obtained  $1.31$  to  $1.91$  times higher than the smooth channel data where detached baffles were installed.

- The friction factor value ( $f$ ) for in which detached baffles were installed was achieved  $2.33$  to  $4.98$  times higher than those of the smooth channel data at the analogous Reynolds numbers.

- The thermal enhancement index ( $\eta$ ) was observed to be around  $0.77$  to  $1.31$  by the channel with detached baffles installed at constant pumping power.

- Installing baffles with floating distance of  $b=0$  at  $Re=9,000$  resulted in thermal enhancement index of  $1.31$  which goes highest when compared to other conditions within this experiment.

- From the past researches conducted, when computational results with less  $b$  values ( $b<2$  millimeters) have been used, heat transfer is more efficient than with  $b=0$  millimeters and as well decreased the pressure drop in test channel. Nevertheless, this conducted research is still unable to control the conditions of the experiment with low  $b$  values due to the standards of installment, resolution of the piece of work used in the experiment, and the measuring equipments that are required to have more efficiency and quality.

### 6. Acknowledgement

The author would like to gratefully acknowledge the Thailand Research Fund (TRF) and the King Mongkut's Institute of Technology Ladkrabang (KMUTL) for the financial support of this research.

### 7. References

#### 7.1 Article in Journals

- [1] M.M.K. Bhuiya, M.S.U. Chowdhury, M. Shahabuddin, M. Saha, L.A. Memon, Thermal characteristics in a heat exchanger tube fitted with triple twisted tape inserts, International Communications in Heat and Mass transfer 48 (2013) 124–132.
- [2] A. Dewan, P. Mahanta, K.S. Raju, P.S. Kumar, Review of passive heat transfer augmentation techniques, Proceedings of the Institution of

## TSF0013

Mechanical Engineers Part A Journal of Power and Energy 218 (7) (2004) 509–527.

[3] S. Liu, M. Sakr, A comprehensive review on passive heat transfer enhancements in pipe exchangers, Renewable and Sustainable Energy Reviews 19 (2013) 64–81.

[4] E. A. M. Elshafei, M. Safwat Mohamed, H. Mansour, M. Sakr, Experimental study of heat transfer in pulsating turbulent flow in a pipe, International Journal of Heat and Fluid Flow 29 (2008) 1029–1038.

[5] S. Seghir-Ouali, D. Saury, S. Harmand, O. Phillipart, D. Laloy, Convective heat transfer inside a rotating cylinder with an axial air flow, International Journal of Thermal Sciences 45 (2006) 1166–1178.

[6] R. Veerapandi, G. Karthikeyanb, G. R. Jinuc, R. Kannaiah, Experimental study and analysis of flow induced vibration in a pipeline, International Journal of Engineering Research & Technology (IJERT) 3 (5) (2014) 1996–1999.

[7] H.A. ATTIA, Unsteady MHD Couette Flow with Heat Transfer in the Presence of Uniform Suction and Injection, Mechanics and Mechanical Engineering 12 (2) (2008) 165-176.

[8] R. S. R. Gorla, J. E. Gatica, B. Ghorashi, P. In-Eure, L. W. Byrd, Heat transfer in a thin liquid film in the presence of electric field for non-isothermal interfacial condition, International Journal of Fluid Mechanics 29 (2002) 146-157.

[9] H.Y. Kim, B.H. Kang, Effects of hydrophilic surface treatment on evaporation heat transfer at the outside wall of horizontal tubes, Applied Thermal Engineering 23 (2003) 449–458.

[10] C.B. Pawar, K.R. Aharwal, A. Chaube, Heat transfer and fluid flow characteristics of rib-groove roughened solar air heater ducts, Indian Journal of Science and Technology 2 (11) (2009) 50-54.

[11] A. Hasan, K. Siren, Performance investigation of plain and finned tube evaporatively cooled heat exchangers, Applied Thermal Engineering 23 (2003) 325–340.

[12] S. Eiamsa-ard, P. Promvonge, Enhancement of Heat Transfer in a Circular Wavy-surfaced Tube with a Helical-tape Insert, International Energy Journal 8 (2007) 29-36.

[13] S. Senthilraja, KCK. Vijayakumar, Analysis of Heat Transfer Coefficient of CuO/Water Nanofluid using Double Pipe Heat Exchanger, International Journal of Engineering Research and Technology 6 (5) (2013) 675-680.

[14] S.D.Patil, A.M. Patil, Analysis of Twisted Tape with Winglets to Improve the Thermohydraulic Performance of Tube in Tube heat exchanger, International Journal of Advanced Engineering Research and Studies 1 (1) (2011) 127-130.

[15] A. Alamgholilou, E. Esmaeilzadeh, Experimental investigation on hydrodynamics and heat transfer of fluid flow into channel for cooling of rectangular ribs by passive and EHD active enhancement methods, Experimental Thermal and Fluid Science 38 (2012) 61–73.

[16] P. Promvonge, C. Thianpong, Thermal performance assessment of turbulent channel flows over different shaped ribs, International Communications in Heat and Mass Transfer 35 (2008) 1327-1334.

[17] A. Kumar, J.L. Bhagoria, R.M. Sarviya, Heat transfer and friction correlations for artificially roughened solar air heater duct with discrete W-shaped ribs, Energy Conversion and Management 50 (8) (2009) 2106-2117.

[18] V. SriHarsha, S.V. Prabhu, R.P. Vedula, Influence of rib height on the local heat transfer distribution and pressure drop in a square channel with 90o continuous and 60o V-broken ribs, Applied Thermal Engineering 29 (2009) 2444-2459.

### 7.2 Books

[19] A. Standard, Measurement of fluid flow in pipes using orifice, nozzle and venturi, ASME MFC-3M, United Engineering Center, 345 East 47th Street, New York, (1984) 1-56.

[20] E. Ower, R.C. Pankhurst, Measurement of Air Flow, Fifth edition Pergamon Press, 1977. (in SI units ed.).

[21] F.P. Incropera, P.D. Dewitt, T.L. Bergman, A.S Lavine, Fundamentals of heat and mass transfer, John Wiley & Sons Inc, 2006.

[22] ANSI/ASME, Measurement uncertainty, PTC 19, 1-1985. Part 1, 1986.